processes

MDPI

Article

Phenol Degradation Kinetics by Free and Immobilized *Pseudomonas putida* BCRC 14365 in Batch and Continuous-Flow Bioreactors

Yen-Hui Lin * and Yu-Siang Cheng

Department of Safety, Health and Environmental Engineering, Central Taiwan University of Science and Technology, 666, Bu-zih Road, Bei-tun District, Taichung 406053, Taiwan; show88567@gmail.com

* Correspondence: yhlin1@ctust.edu.tw; Tel.: +886-4-22391647 (ext. 6861)

Received: 25 May 2020; Accepted: 18 June 2020; Published: 21 June 2020

Abstract: Phenol degradation by *Pseudomonas putida* BCRC 14365 was investigated at 30 °C and a pH of 5.0–9.0 in the batch tests. Experimental results for both free and immobilized cells demonstrated that a maximum phenol degradation rate occurred at an initial pH of 7. The peak value of phenol degradation rates by the free and immobilized cells were 2.84 and 2.64 mg/L-h, respectively. Considering the culture at 20 °C, there was a lag period of approximately 44 h prior to the start of the phenol degradation for both free and immobilized cells. At the temperatures ranging from 25 to 40 °C, the immobilized cells had a higher rate of phenol degradation compared to the free cells. Moreover, the removal efficiencies of phenol degradation at the final stage were 59.3–92% and 87.5–92%, for the free and immobilized cells, respectively. The optimal temperature was 30 °C for free and immobilized cells. In the batch experiments with various initial phenol concentrations of 68.3–563.4 mg/L, the lag phase was practically negligible, and a logarithmic growth phase of a particular duration was observed from the beginning of the culture. The specific growth rate (μ) in the exponential growth phase was 0.085–0.192 h^{-1} at various initial phenol concentrations between 68.3 and 563.4 mg/L. Comparing experimental data with the Haldane kinetics, the biokinetic parameters, namely, maximum specific growth rate (μ_{max}), the phenol half-saturation constant (K_s) and the phenol inhibition constant (K_I), were determined to equal 0.31 h^{-1}, 26.2 mg/L and 255.0 mg/L, respectively. The growth yield and decay coefficient of *P. putida* cells were $0.592 \pm 4.995 \times 10^{-3}$ mg cell/mg phenol and $5.70 \times 10^{-2} \pm 1.122 \times 10^{-3}$ day^{-1}, respectively. A completely mixed and continuous-flow bioreactor with immobilized cells was set up to conduct the verification of the kinetic model system. The removal efficiency for phenol in the continuous-flow bioreactor was approximately 97.7% at a steady-state condition. The experimental and simulated methodology used in this work can be applied, in the design of an immobilized cell process, by various industries for phenol-containing wastewater treatment.

Keywords: phenol degradation; kinetics; *Pseudomonas putida*; batch experiments; continuous-flow bioreactor

1. Introduction

Phenols, such as xenobiotic contaminants, emerge from various anthropogenic activities due to industrialization, and are often found in different environmental conditions [1,2], such as surface waters, wastewater, groundwater and sludge products [3–5]. Phenol, as a major component present in the effluents from several industries (oil refineries, coking plants, steel industries, etc.), has been reported to be very harmful to the aquatic ecosystem [6,7]. The saline water in the Port of Gotherburg, located on the west coast of Sweden, was contaminated by a chemical spill of hundreds of tons of phenol in 1973 [8]. Additionally, several phenol leakage spills that occurred in Korea were also reported [9]. As a result, phenol is considered as a highly toxic and deleterious compound in accidental chemical spills,

according to Korea's Chemicals Control Act [9]. Regulations of US Environmental Protection Agency (USEPA) limit the phenol concentration in surface waters to below 1 μg L^{-1} (ppb) [8]. The discharge limit of phenol concentration in wastewater released into surface water should be less than 1 mg L^{-1}, according to USEPA regulations [10]. Phenols as environmental pollutants are hazardous to human health and living organisms, owing to their high toxicity levels, and their suspected carcinogensas well as mutagenic impacts on cells [11]. Phenol at low concentrations of 5–25 mg L^{-1} poses a potential carcinogenic risk to human beings, and is fatal to fishes [12]. Several studies found that opossum shrimp and carp, as marine and freshwater organisms, respectively, had the most sensitivity to phenol [13,14]. The toxicity tests revealed that the lethal concentration 50 (LC50) of phenol for opossum shrimp and carp was 1.555 mg/L and 0.26 mg/L, respectively, for 96 h [13,14]. Thus, the removal of phenol from water and wastewater is an urgent task to protect our natural water resources.

The phenolic compounds can be treated by various physical, chemical and biological methods, such as adsorption by activated carbon, chemical decomposition, and biodegradation [15]. Among those methods, aerobic biodegradation has been considered as the best approach to treat phenolic compounds because it is an environmentally friendly and cost-effective method. The strain of *Pseudomonas putida* (*P. putida*) with a high capacity for degrading phenol is well-known. Many researchers have focused on the study of aerobic biodegradation of phenol by *P. putida* under a suspended or immobilized state. Parvanova-Mancheva et al. [16] conducted a batch bioreactor to evaluate phenol degradation by *P. putida*, and found that an initial phenol concentration of 1.9 g L^{-1} was completely degraded after an operational time of 23 days. Kurzbaum et al. [17] encapsulated *P. putida* cells in small bioreactor platform capsule to observe the phenol degradation. Their experimental results indicated that phenol with an initial concentration of 800 mg L^{-1} was completely consumed by free or encapsulated cells. The bubble column and spouted bed bioreactors, with *P. putida* cells within polyvinyl alcohol (PVA), were successfully conductedto remove phenol from simulated wastewater [18]. Dong et al. [7] developed a nanocomposite that immobilize *P. putida* cells in order to remove phenol effectively. The results of batch experiments revealed that the initial phenol concentrations at 10 and 20 mg/L were completely degraded, at time courses of 13 and 24 h, respectively [7].

Conventional suspended-growth treatments are easily inhibited by toxic phenol, and biomass is readily lost from the bioreactor. Hence, the immobilization of cells in gel beads has become an attractive technique for the biodegradation of toxic phenolic compounds [19]. Immobilized microorganism technology is being increasingly used for the elimination of organic pollutants from contaminated environments [20]. Immobilization is the restriction of cell mobility within a defined space. Natural polymers, such as calcium alginate, chitin, chitosan as well as cellulose derivatives, were used as the matrices for cell immobilization [21,22]. Immobilized cell cultures exhibit potential advantages over suspended-growth cultures; cell immobilization provides a higher cell concentration, cell recyclability, and the elimination of costly processes for cell recovery. In addition, the fixed and fluidized bed bioreactors with immobilized cells exhibit a lower susceptibility to clogging under continuous-flow conditions, which is a convenience for regeneration, the reusability of cells, and solid–liquid separation [23].

The aim of this study was to perform a continuous-flow moving-bed bioreactor with immobilized *P. putida* cells, to deal with synthetic phenol-containing wastewater with optimal pH and temperature under aerobic conditions. In the steady state, the feed phenol concentration was gradually increased up to 1000 mg/L, in order to evaluate the degree of phenol removal efficiency at various phenol organic loading rates. The objectives of this study were to (1) use free and immobilized cells to degrade phenol, in order to determine the optimal pH and temperature; (2) observe phenol biodegradation with the growth of free *P. putida* cells in different batch experiments, in order to determine the biokinetic parameters (K_S, K_I, $Y_{X/S}$ and b) at optimal pH and temperature; (3) propose a kinetic model system of the immobilized cells in the continuous-flow moving-bed bioreactor; (4) conduct a continuous-flow moving-bed bioreactor with immobilized cells to verify the model at optimal pH and temperature.

2. Model Description

2.1. Model Assumptions

The theoretical concentration profile of phenol in bulk liquid phase, liquid film phase and gel bead phase was assumed (Figure 1). In order to model phenol biodegradation kinetics by immobilized cells, the following assumptions are made: (1) all beads are spherical in shape; (2) the mass transfer phenomenon of phenol from liquid film phase to gel bead phase is dominated by Fick's law; (3) phenol is migrated from bulk liquid phase to the gel bead phase through the liquid film by molecular diffusion; (4) the cells are distributed uniformly in the gel bead; (5) all phenol concentrations in the bulk liquid are the same; and (6) the effects of suspended cells in the bulk liquid phase are insignificant.

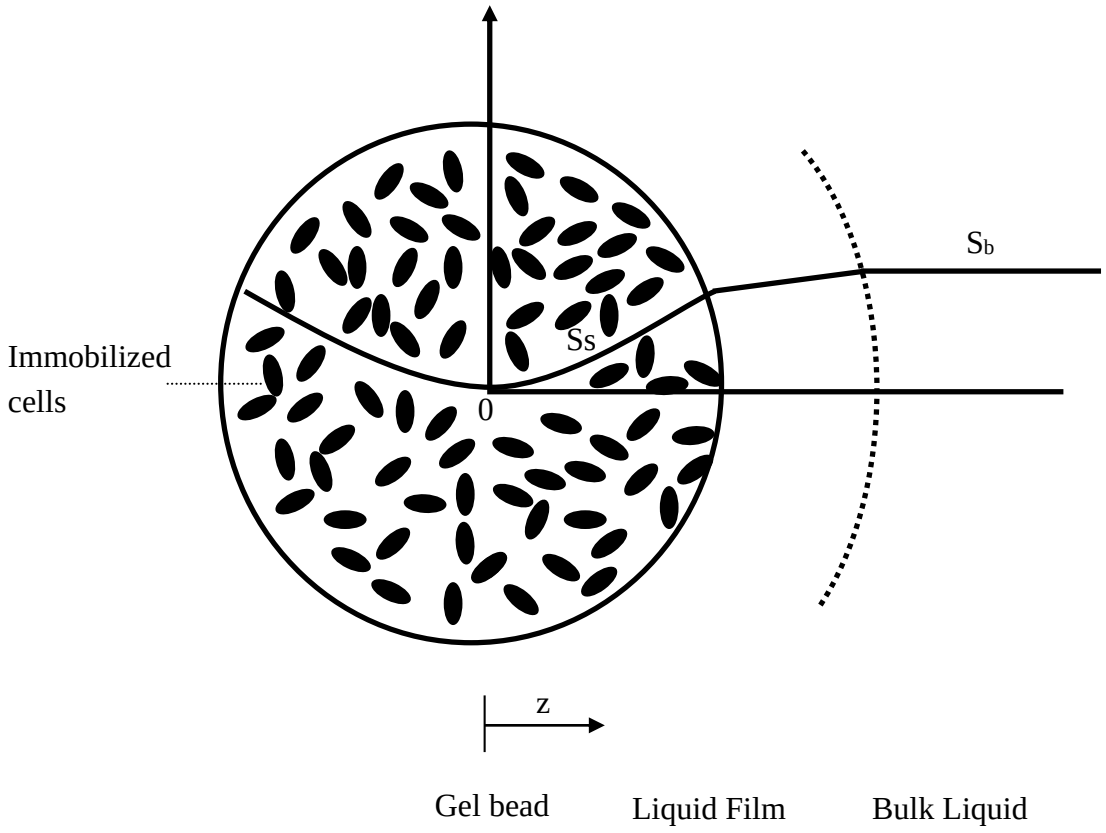

Figure 1. Concentration profile of phenol in an immobilized cell system.

2.2. Kinetic Model in the Immobilized Cells

When the immobilized cells are used for biodegradation, the phenol diffuses into the gel beads and is degraded by the immobilized cells in the calcium alginate. The homogenous solid diffusion and biodegradation by immobilized cells take place in this case. The phenol utilization rate in the spherical granule is equal to the homogeneous solid diffusion rate combined with the biological reaction rate in the spherical granule at an unsteady state [24]:

$$\frac{\partial S_s}{\partial t} = D_e\left(\frac{\partial^2 S_s}{\partial z^2} + \frac{2}{z}\frac{\partial S_s}{\partial z}\right) - r_s \quad (1)$$

where S_s is the phenol concentration within the gel beads (mg L^{-1}), D_e is the effective diffusivity of the phenol within the porous matrix (cm^2 d^{-1}), z is the radial coordinate within the beads, and r_s is the phenol utilization rate by immobilized cells (mg L^{-1} d^{-1}). The phenol utilization rate (r_s) is a function of the phenol concentration, as well as the cell density (X_s).

Since phenol can be degraded by *P. putida* cells as a sole carbon source, and presents cell growth inhibition, the phenol utilization rate (r_s) in the spherical granule [Equation (1)] was expressed by the Haldane equation as follows [25]:

$$r_s = -\frac{\mu X}{Y_{X/S}} = -\frac{\mu_{\max} X_s S_s}{Y_{X/S}\left(K_s + S_s + S_s^2/K_{\mathrm{I}}\right)} \tag{2}$$

where μ is the specific growth rate (day^{-1}), $\mu_{\max}$ represents the maximum growth rate (day^{-1}), $Y_{X/S}$ is the growth yield of cells (mg mg^{-1}), K_s is the substrate-affinity constant (mg L^{-1}), S_s is the phenol concentration in the beads (mg L^{-1}), X_s is the cell concentration in the beads (mg cell L^{-1}), and K_I is the substrate-inhibition constant (mg L^{-1}). A larger K_I value denotes that the cell is less sensitive to phenol inhibition [26].

The growth rate of cells in the beads can be expressed by the following equation:

$$\frac{\partial X_s}{\partial t} = (\mu - b) X_s \tag{3}$$

where b is the endogenous decay coefficient of cells (d^{-1}).

The mass balance of substrate in the bulk liquid can be expressed by the following:

$$\frac{dS_b}{dt} = \frac{Q}{V\varepsilon}(S_{b0} - S_b) - k_f a V_s (S_b - S_s)\ z = R \tag{4}$$

where S_b is the phenol concentration in the bulk liquid (mg L^{-1}), D_e is the effective diffusivity of phenol in the gel beads (cm^2 d^{-1}), k_f is the mass transfer coefficient of phenol (cm d^{-1}), a is the specific surface area based on the total reactor volume (cm^{-1}), and V_s is the beads volume per unit reactor volume (dimensionless). At the start of the phenol's biodegradation by the immobilized cells, the beads are devoid of phenol, and the cells are assumed to be evenly distributed in the beads. The initial conditions can be expressed as follows:

$$\mathrm{IC1}:\ S_s = 0\ 0 \le z \le R,\ t = 0 \tag{5}$$

$$\mathrm{IC2}:\ X_s = X_0\ 0 \le z \le R,\ t = 0 \tag{6}$$

The flux diffusing from the liquid film into the interface is equal to the flux diffusing out of the interface and into the beads. The boundary conditions for the mass transfer can be found at the bead/liquid interface, and can be described as follows:

$$\mathrm{BC1}:\ \frac{\partial S_s}{\partial z} = 0\ z = 0 \tag{7}$$

$$\mathrm{BC2}:\ D_e \frac{\partial S_s}{\partial z} = k_f (S_b - S_s)\ z = R \tag{8}$$

2.3. Model Numerical Solution

Equations (1)–(8) constitute an immobilized cell model system for phenol biodegradation in a continuous-flow bioreactor. The orthogonal collocation method (OCM) and Gear's method were used to solve the immobilized cell kinetic model [27]. The continuous-flow immobilized cells equations were first normalized by denoting the dimensionless variables. The Legendre polynomial, as an even function in the spherical coordinate, was applied to estimate the exact phenol concentration profile of the beads. The roots of the Legendre polynomial are used as collocation points that are not equally allocated in the domain. The collocation points distributed in the beads wereset at 6. Six ordinary differential equations were formed from a conversion of the nonlinear parabolic differential equation (Equation (1)). The immobilized cell kinetic model, containing the eight ordinary differential equations, was integrated by Gear's method to calculate the phenol concentration profile, immobilized cells growth, the phenol

concentration in effluent and the flux diffused into the beads. All main and subroutine programs written in Fortran language were compiled, linked and executed with a Macintosh computer.

2.4. Evaluation of Biokinetic Parameters

The specific growth rate of *P. putida* cells in the exponential phase in a batch system, μ (h^{-1}), is defined as follows [28,29]:

$$\mu = \frac{1}{X}\frac{dX}{dt} = \frac{d\ln X}{dt} \tag{9}$$

where X is the cell concentration (mg/L or O.D.). Integration and simplification of Equation (9) yields the following relationship:

$$\mu = \frac{\ln(X_2/X_1)}{t_2 - t_1} \tag{10}$$

where X_1 and X_2 are the cell concentrations at times t_1 and t_2, respectively. The value of μ can thus be calculated from the slope of ln$X$ against time in the exponential growth phase of the curve.

The growth yield of cells was determined from the slope of the cells produced against phenol consumption, by performing linear regression via the following equation:

$$Y_{X/S} = \frac{X_t - X_0}{S_0 - S_t} \tag{11}$$

where $Y_{X/S}$ is the growth yield of *P. putida* cells (mg cell/mg phenol), X_0 and X_t are cell concentrations at times zero and t; and S_0 and S_t are the phenol concentrations at times zero and t.

The growth curve of *P. putida* cells shows an endogenous phase in the batch experiments. The experimental data in the declining phase was used to evaluate the decay coefficient (b) of cells. The decay coefficient (b) can be expressed by the following equation [30]:

$$b = -\frac{\ln(X_2/X_1)}{t_2 - t_1} \tag{12}$$

where X_1 and X_2 are cell concentrations at times t_1 and t_2, respectively.

2.5. Mass Transfer Coefficients

A random pore empirical formula was applied to derive the effective diffusivity for diffusion under the reaction conditions [31]. Furthermore, the random pore model is a notable predictor of galactose effective diffusivity in the immobilized cell system, which has been proven by Korgel et al. [32]. According to this formula, the effective diffusivity (D_e) is estimated by

$$D_e = D_s(1 - \alpha X)^2 \tag{13}$$

where D_s is the diffusivity in gel beads without cells. α and X are the specific volume of the *P. putida* cells (L/g) and the *P. putida* cells' concentration (g/L), respectively.

The value of the external mass transfer coefficient k_f is estimated by the following correlation [33]:

$$k_f = \frac{Sh \times D_s}{d_p} \tag{14}$$

where Sh is the Sherwood number = $\{4 + 1.21(Re)^{2/3}(Sc)^{2/3}\}^{1/2}$, Re is Reynolds number = $\rho d_p v_s/\mu$, Sc is Schmidt number = $\mu/\rho D_s$, ρ is the mass density of flowing fluid, d_p is the diameter of the gel beads, and μ is the absolute viscosity of water.

3. Materials and Methods

3.1. Chemicals

All chemicals used in the experiments are analytical grade. Reagent grade Phenol and sodium-alginate were purchased from Sigma Aldrich Ltd., Schnelldorf, Germany. The stock solution was prepared by dissolving 2 g phenol in 1.0 L deionized/distilled water. The test phenol concentrations were determined by diluting 2000 mg L^{-1} of phenol stock solution to the desired concentrations.

3.2. Cultivation of Pseudomonas putida Cells

Pure culture of *Pseudomonas putida* ATCC 14365 was originally obtained from the Food Industry Research and Development Institute (Hsinchu, Taiwan). The freeze-dried culture fixed firmly in a tube was placed in the refrigerator and kept at 4 °C until use. In order to activate suspended cells, the nutrient medium with 0.5 mL was added to the tube to melt the frozen stock culture. The activated cells with nutrient medium were enriched at 30 ± 0.2 °C for 3–4 days to guarantee the viability of *P. putida* cells. In the late-exponential growth phase, the activated cells were harvested as inoculums. The inoculum of cells was then used as a fresh stock culture for batch and continuous-flow experiments. The nutrient medium consisted of 3 g/L of beef extract, as well as 5 g/L peptone, and mineral salt medium (MSM) at a pH of 7. The MSM was composed of the following components (per liter) [34]: 0.42 g of KH_2PO_4, 0.375 g of K_2HPO_4, 0.244 g of $(NH_4)_2SO_4$, 0.015 g of NaCl, 0.015 g of $CaCl_2{\cdot}2H_2O$, 0.05 g of $MgSO_4{\cdot}7H_2O$ and 0.054 g of $FeCl_3{\cdot}6H_2O$. A phosphate buffer (pH 7) was prepared by dissolving 8 g/L of NaCl, 0.2 g/L of KCl, 1.15 g/L of K_2HPO_4 and 0.2 g/L of KH_2PO_4 in deionized distilled water (Millipore, Burlington, MA, USA, Milli-Q) [35]; the nutrient medium and phosphate buffer were sterilized in an autoclave at 121 °C for 15 min prior to use. All inorganic chemicals were purchased from Merck Co. (Taipei, Taiwan) at reagent grade. The inoculum for batch and continuous-flow experiments was prepared according to the methods of Juang and Tsai [34]. *P. putida* cells were activated at 30 °C by adding the salt medium, then 1.0 mM phenol was added for cell enzyme adaption for 24 h. In the late-exponential growth phase, the activated cells were harvested as inocula. The suspended activated cells in each 15-mL centrifugal tube were transported into a centrifuge (Z206 A, Hermle, Wehingen, Germany), and collected after a centrifugation at 6000 rpm for 5 min; this was followed by a resuspension in phosphate buffer and a subsequent centrifuge [35]. Following the cleaning process, an initial cell concentration of 0.109–0.150 optical density (OD) was provided by inoculating the activated cells into the culture medium for a total volume of 180 mL in 250-mL Erlenmeyer flasks. After the inoculation, the flasks were capped and placed into an orbital shaker incubator (JSL-530, Lenon Instruments, Taichung, Taiwan), at 120 rpm and 30 °C for the batch experiments.

3.3. Batch Experiments

Upon the cultivation of *P. putida* cells, the phenol biodegradation by free or immobilized cells at different pH values and temperatures was evaluated to determine the optimal pH and temperature, respectively. In the first batch test, the pH range was 5–9 and the temperature was controlled at 30 °C. In the second batch test, the temperature range was 20–40 °C and pH was maintained at 7. The initial phenol and cell concentration was about 40 mg phenol L^{-1} and 4.13 mg cell L^{-1} (0.012 OD). Furthermore, in the third batch test, seven batch experiments were carried out to evaluate the phenol biodegradation and free cell growth, for determining the biokinetic parameters under optimal pH and temperature. The ratio of initial cell concentration to phenol (S_0/X_0) was in the range of 15.0–35.3 mg phenol/mg cell in the seven batch experiments. Table 1 lists the operational condition in the batch experiments to evaluate biokinetic parameters. The samples were withdrawn at the onset of the batch experiments, and then again at suitable time intervals of 2–10 h, for the measurement of cell density and phenol concentration. Juang and Tsai [34] carried out the several batch experiments to investigate the biodegradation of phenol and the growth of *P. putida* cells. The time intervals for samples withdrawn in their study are similar to those set by this study.

Table 1. Batch kinetic experiments to evaluate biokinetic parameters.

Run No.	Temp. (°C)	pH	Initial Phenol Conc. (mg L^{-1})	Initial Cell Conc. (mg cell L^{-1})	Culture Duration (h)
1	30	7.0	68.3	4.1	95
2	30	7.0	95.2	5.8	99
3	30	7.0	133.0	6.9	101
4	30	7.0	258.7	7.3	101
5	30	7.0	320.5	21.4	117
6	30	7.0	332.4	14.9	117
7	30	7.0	563.4	20.4	432

3.4. Immobilization Protocol

In the late-logarithmic phase of the cell growth curve, *P. putida* was collected and centrifuged then re-suspended in 15 mL of 3% (*w*/*w*) sodium alginate according to the method provided by Chung et al. [36]. This mixture was gravitationally dribbled into 1% (*w*/*v*) $CaCl_2$ solution using syringe No. 16. The drops of the sodium alginate were gelled to form constant and definite-sized beads upon contact with the $CaCl_2$ solution. These spherical gel beads were obtained by the immobilization method with an average size of 3 mm.

3.5. Analysis of P. putida Cells and Phenol

Cell density was measured at 600 nm using an UV/Vis spectrophotometer. The measurement of an optical density (OD) below 0.70, by diluting the samples, was to follow the Beer–Lambert law [25]. The OD value was then converted to dry cell density using a dry weight calibration curve. The values of OD600 were converted to cell density by the following linear regression: X (mg/L) = 343.75 (OD_{600}). A 0.7 mL sample was filtered through a 0.2-µm Millipore syringe filter and subjected to phenol analyses. High performance liquid chromatography (HPLC), by Alliance 2695 (Waters Co., Miford, MA, USA), was used to analyze the phenol concentration. The HPLC contained the autosampler of Waters 2707, and a Waters 2487 UV/Vis detector of Waters 2487. The HPLC system was equipped with a 150 × 3.9-mm Symmetry® C18 column packing with a particle size of 5 µm. The samples were eluted at a flow rate of 0.7 mL/min with a mobile phase consisted of 50 mM potassium phosphate/acetonitrile (70/30, *v*/*v*) for 8 min. The UV/Vis spectrophotometric detector was fixed at 254 nm. The injection volume of each sample was 6 µL. Reproducibility of the concentration measurements was within 5% [36]. The concentrations of phenol were determined by following linear regression equation: Phenol (mg/L) = $3.1992 + 3 \times 10^{-4} \times$ (Area), $R^2 = 0.9998$.

3.6. Bioreactor Setup

An up-flow moving-bed immobilized cell bioreactor is provided in Figure 2; the system is circular in shape and made of Plexiglas. This immobilized-cell bioreactor is 10 cm in diameter and 46.6 cm in height, with a liquid level of 29.5 cm, giving a total volume of 2.55 L and a working volume of 1.568 L, which yielded a 6-h hydraulic retention time (HRT). Approximately 50% of the working volume (i.e., 0.784 L) was filled with Ca-alginate beads 3 mm in diameter. The required oxygen for the system is supplied by one air plate connected to an air aquarium compressor with output air capacity of 2 L/min so that the dissolved oxygen and gel bead motions were sufficient [37]. A single plastic sieve was placed at the bottom of the reactor to hold the air plate in place. The substrate was fed by a peristaltic pump (Masterflex, Cole Parmer Instrument Company, Chicago, IL, USA) from the right side of the reactor. The temperature of immobilized cell bioreactor was controlled at 30 ± 0.2 °C with a water jacket connected to a circulating water bath (Yih Der Inc., Taipei, Taiwan). The pH was buffered at 7.0 ± 0.2 by HPO_4^{2-}/H_2PO4^- in the feed solution.

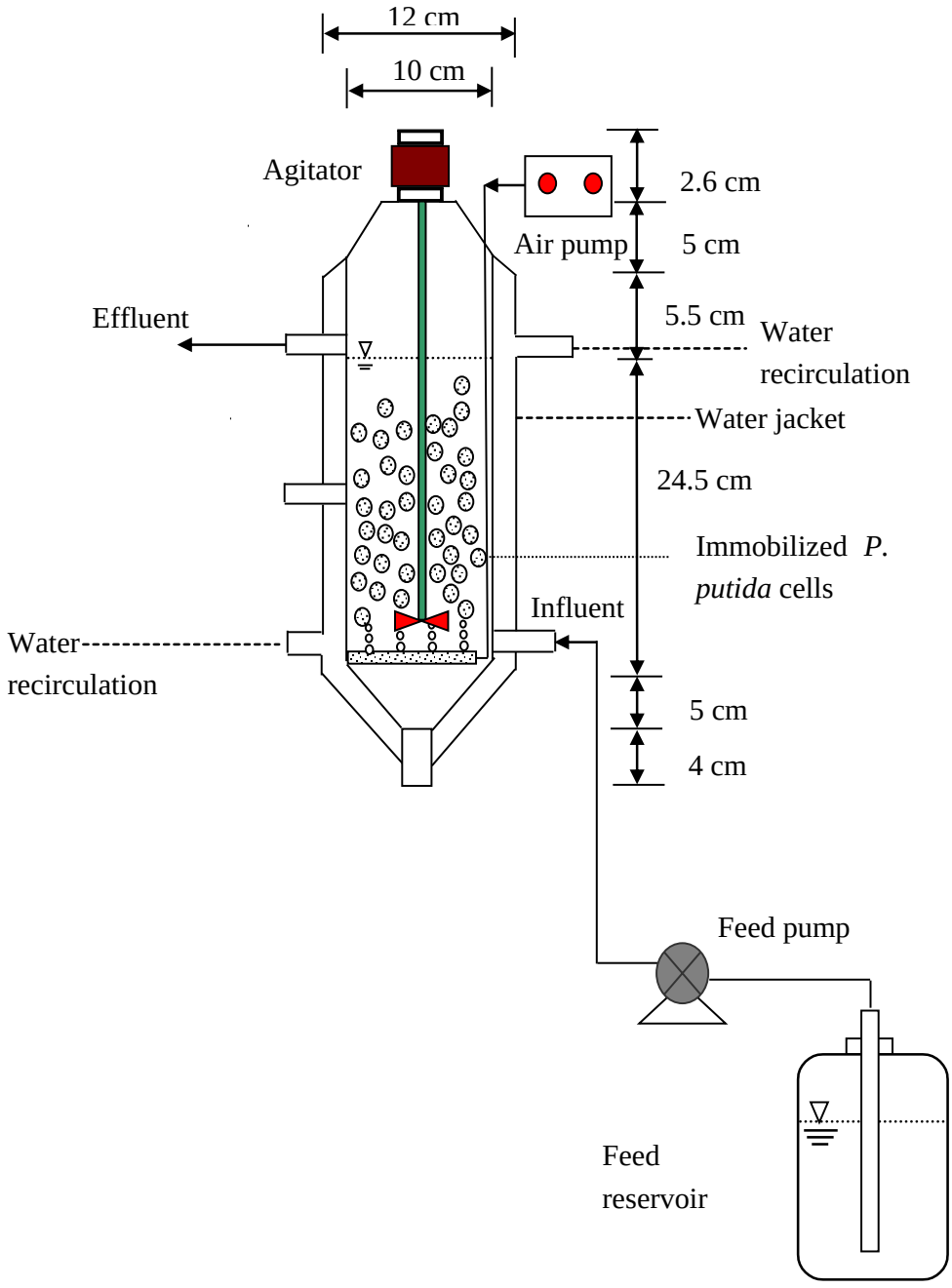

Figure 2. A continuous-flow immobilized cell reactor setup.

4. Results and Discussion

4.1. Phenol Degradation by Free and Immobilized Cells

Figure 3 presents the effect of pH on phenol degradation by free and immobilized cells over 53.5 h, at an initial pH range of 5–9, and at 30 °C. The phenol degradation rapidly decreased during the initial 8 h at various initial pH values. The decline in phenol degradation became more gentle after 8 h. The phenol degradation trend by free and immobilized cells under different initial pH values was similar. The immobilized cells had a slightly higher phenol utilization rate than that of the free cells, as the system shifted to having a more acidic pH (5.0). However, the free cells showed a higher phenol degradation rate than that of immobilized cells at an initial pH of 6–9. Experimental results demonstrated that the maximum phenol degradation rate occurred at an initial pH of 7 for both free

and immobilized cells. The peak values of phenol degradation by the free and immobilized cells were 2.84 and 2.64 mg/L-h, respectively, at optimal pH of 7.

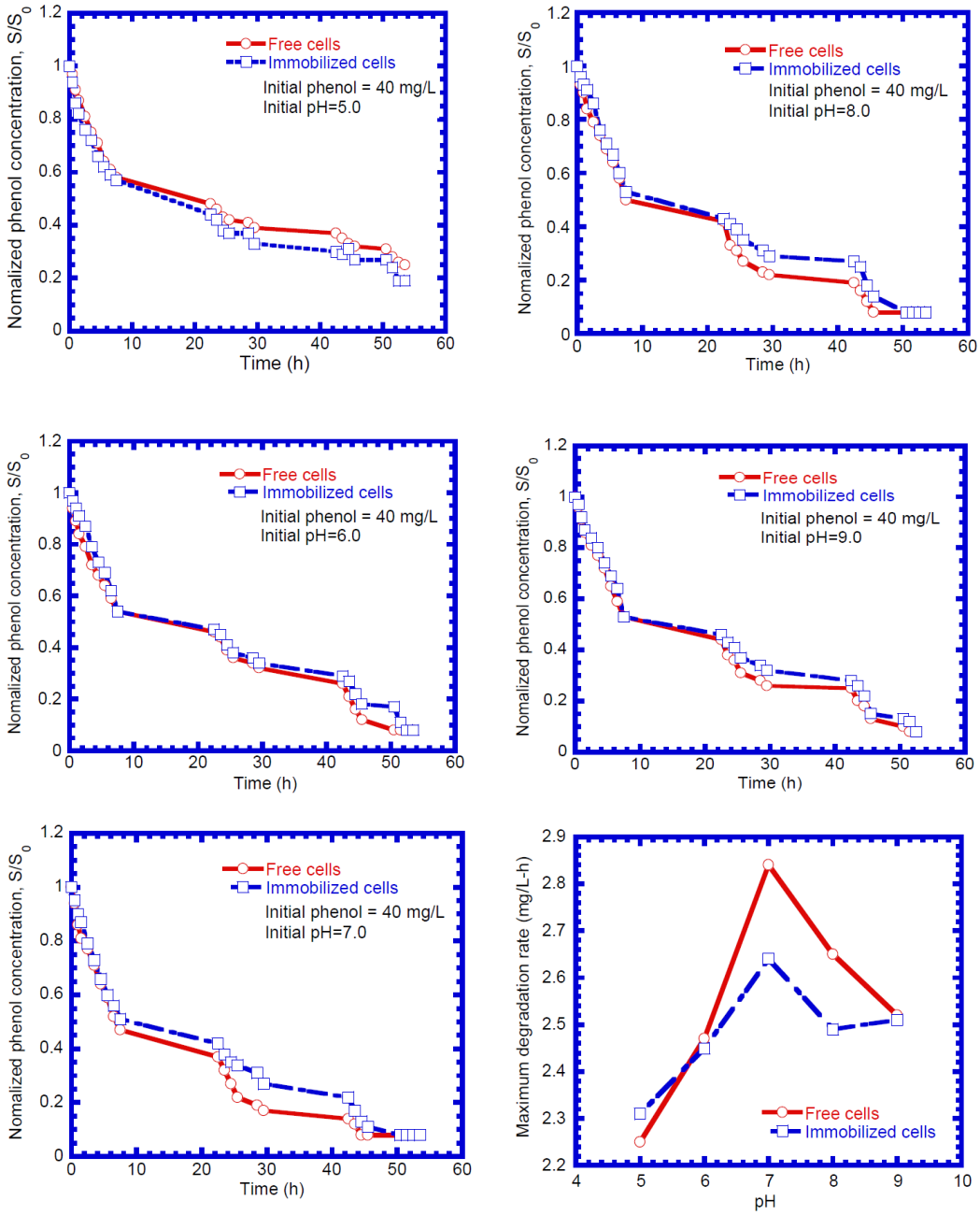

Figure 3. Effect of pH on phenol degradation by free and immobilized cells.

Figure 4 shows the influence of temperature on phenol degradation by free and immobilized cells. At a culture temperature of 20 °C, the lag period for the start of phenol degradation is approximately 44 h for the free and immobilized cells. The trend of the phenol concentration curves was similar for both cases; however, the maximum phenol degradation rates were 0.816 and 0.560 mg/L-h for free and immobilized cells, respectively. At the temperature range of 25–40 °C, at pH 7, the immobilized cells had a higher phenol degradation than that of free cells, and the removal efficiencies of phenol degradation at the final stage were 59.3–92% and 87.5–92%, for the free and immobilized cells, respectively. The optimal temperature was 30 °C for both free and immobilized cells, with the highest phenol removal efficiency of 92%.

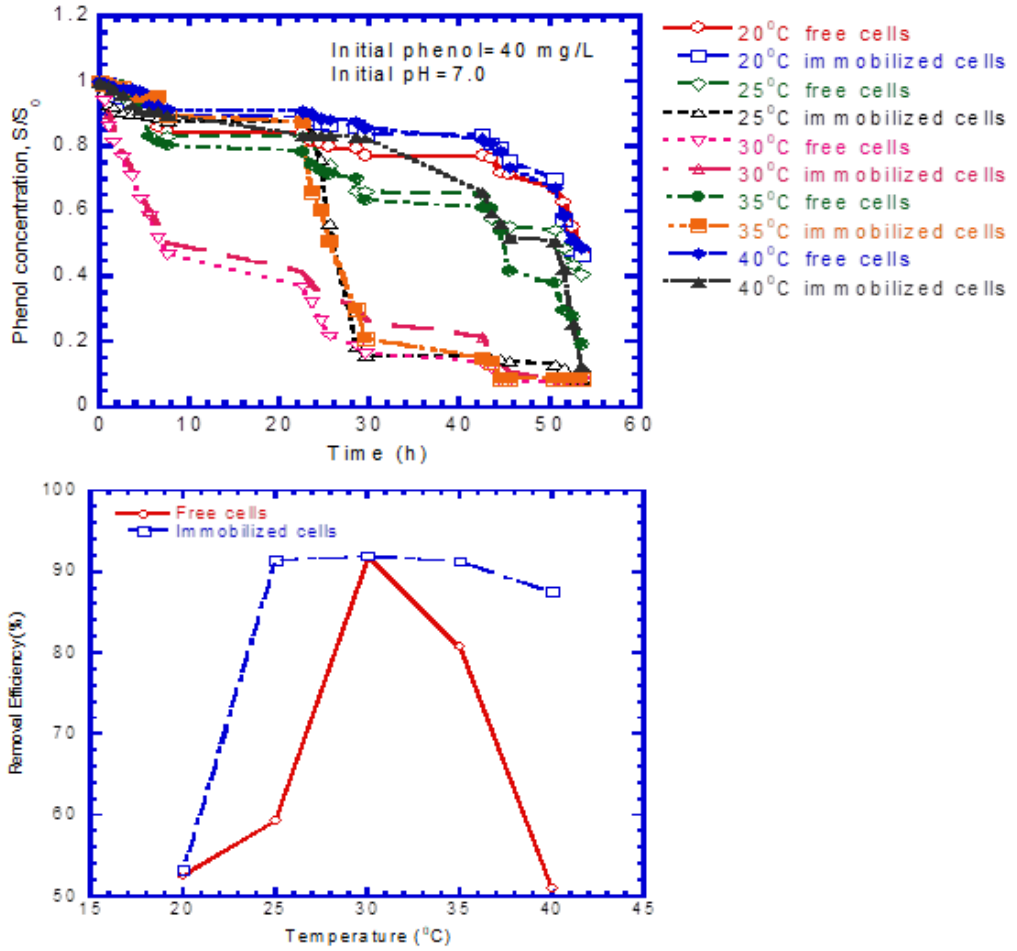

Figure 4. Effect of temperature on phenol degradation by free and immobilized cells.

4.2. Batch Experiments for Free Cells

The phenol biodegradation and cell growth, using phenol-adapted cells as an inoculum and at various initial phenol concentrations of 68.3–332.4 mg/L, is shown in Figure 5. The decrease in phenol content was steeper with higher initial phenol content. The time required for the complete biodegradation of phenol was apparently less than 100 h at lower phenol concentrations (133.0 mg/L), however, the time required for the complete consumption of phenol (i.e., removal efficiency = 100%) was approximately 100–120 h (Figure 5a). Chung et al. [36] reported that the complete biodegradation of 95–400 mg/L phenol took approximately 6–20 h in the batch experiments. Moreover, Rosenkranz et al. [38] assessed the phenol biodegradation efficiency and evaluated the variations in microbial community shift with increasing phenol concentrations, from 120 to 1200 mg/L, in an anaerobic sequencing batch reactor (SBR). Their experimental results showed that the reaction time required for complete removal of inlet phenol (120–1200 mg L^{-1}) was 13–220 h. Vital-Jacome et al. [39] operated an aerobic SBR with granular sludge to degrade 4-chlorophenol-containing synthetic wastewater. In the first three cycles, the complete removal of 4-chlorophenol at reaction times of 84, 8 and 6 h, respectively, was achieved in their study. Kamali et al. [6] indicated that the initial phenol concentration of 250–1000 mg/L was nearly degraded within 150–390 min in an aerobic SBR with the well-acclimated, activated sludge mixed culture. Later on, Angelucci et al. [40] conducted an anaerobic SBR with a stepwise increase in phenol concentration, from 100 to 2000 mg/L, in order to induce a specialized microbial consortium for phenol degradation. They found that the initial phenol concentration of 1000 mg/L was completely removed after 10 days. In this study, the maximum phenol degradation rate ranged from 0.190 to 0.725 g phenol g $cell^{-1}d^{-1}$ when the initial phenol concentration was increased

from 68.3 to 563.4 mg L^{-1}. This finding was much higher than that (0.011 g phenol $gVSS^{-1}d^{-1}$) obtained in the study of Rosenkranz et al. [38]. However, the value of the maximum phenol degradation rate attained in this study was much lower compared to that (12.5 g phenol $gVSS^{-1}$ d^{-1}) reported by Kamali et al. [6].

The cell growth profiles under different initial phenol concentrations are shown in Figure 5b. The *P. putida* cells' concentration gradually increased between 20 and 100 h, when the phenol was gently degraded to depletion. The cell concentration ranged from 0.012 to 0.573 OD_{600} (4.13–196.97 mg cell/L) over a wide range of various initial phenol concentrations (68.3–332.4 mg/L). No lag phase was observed from the beginning of the cell growth, although the initial phenol concentration increased up to 332.4 mg/L with an initial cell concentration of 0.043 OD_{600} (14.78 mg cell/L). This indicated that the *P. putida* cells adapted with the 1.0 mM phenol had an enhanced ability to degrade higher phenol concentrations [34]. Figure 6 presents the variation in phenol and cell concentrations over time, with an initial phenol concentration of 563.4 mg/L and a cell concentration of 0.059 OD_{600} (20.28 mg cell/L). Phenol degradation and cell growth were initiated with a lack of the lag phase. This result was consistent with that reported by Sahinkaya and Dilek [41], who reported that the lag phase disappeared following the acclimationof the culture. Experimental results revealed that the time needed for the complete degradation of phenol was approximately 432 h in this study. Experimental data regarding the *P. putida* cells presented a typical growth and decay curve, observed from a well-defined growth phase and an endogenous phase [42]. The *P. putida* cell concentration of maximal growth was 0.751 OD_{600} (258.16 mg cell/L). The concentration data of phenol and *P. putida* cells adhered to the prior estimations of the biokinetic constants for evaluating the phenol degradation rate along with the growth rate of *P. putida* cells. The relevant techniques employed to determine the biokinetic parameters from the experimental data of the batch experiments are discussed below.

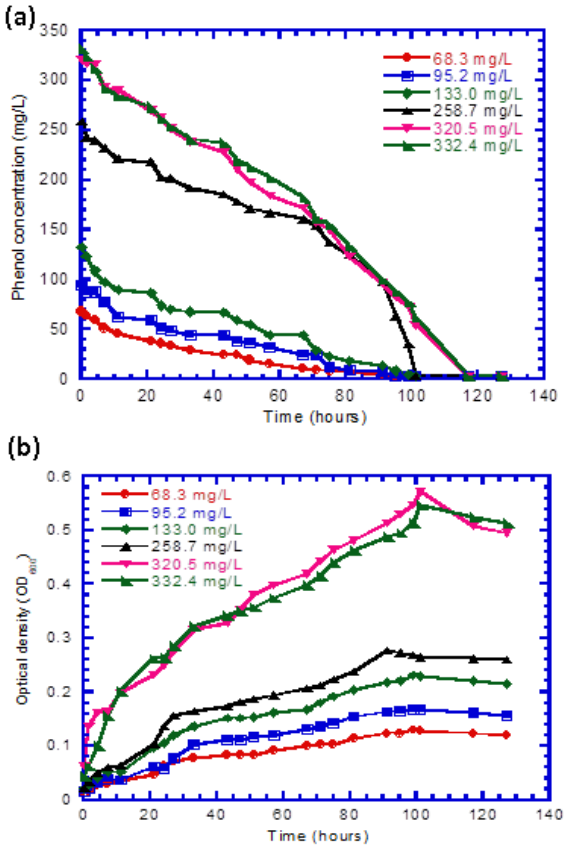

Figure 5. Batch kinetic tests for phenol degradation and cell growth: (**a**) phenol (**b**) *P. Putida* cells.

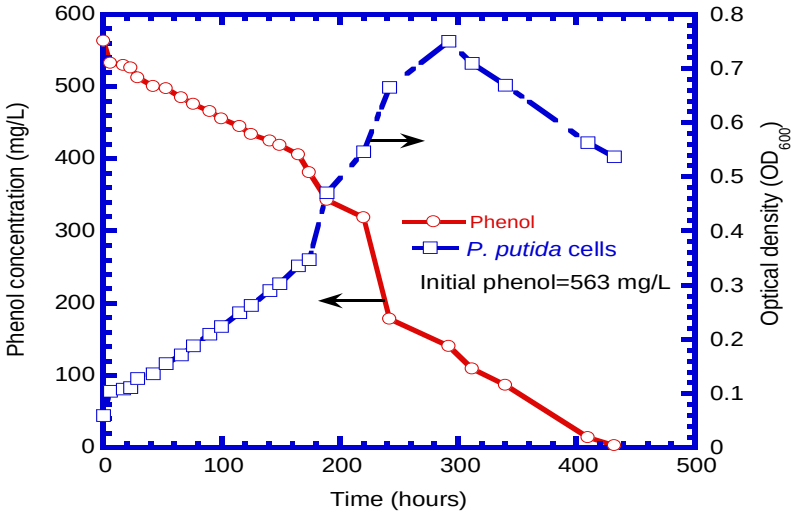

Figure 6. Batch kinetic test for phenol degradation and cell growth.

4.3. Determination of Biokinetic Parameters

Figure 7 shows the time profile of the growth curve for determining a specific growth rate at the logarithmic growth phase for each batch test, at various initial phenol contents ranging from 68.3 to 563.4 mg/L, and initial cell concentrations ranging from 0.012 to 0.059 OD_{600} (4.13–20.28 mg cell/L). The range of the specific growth rate obtained from seven batch experiments was 0.093–0.192 h^{-1}.

Figure 8 presents the specific growth rate, which varied with initial phenol concentrations. The Haldane kinetics were fitted to the obtained data, by using a least-square methodology to determine the values of μ_{max}, K_s and K_I, which were 0.31 h^{-1} (7.44 d^{-1}), 26.2 mg/L and 255.0 mg/L, respectively. Therefore, the observed kinetic equation was determined as follows:

$$\mu = \frac{0.31S}{26.2 + S + S^2/255.0} \quad (15)$$

Table 2 lists the biokinetic parameters obtained from this study and the published data from the literature. A value of μ_{max}, obtained from various aerobic studies, within 0.051–0.9000 h^{-1} range was reported in the existing literature. *P. putida* ATCC 49451 had the highest value of μ_{max} among those different cultures listed. The value of μ_{max} (0.31 h^{-1}) obtained from this study was close to that reported by Chung et al. [36]. In addition, the μ_{max} value of our pure culture was comparable to that of the mixed culture used by Bajaj et al. [43]. The K_S value in this study falls into the range of 6.19–692 at different aerobic conditions. The present K_S value was higher than that in the literature, ranging from 6.19–18 mg/L due to the use of different initial phenol concentrations and culture media [25,36,44,45]. The anaerobic microbial system had a much higher K_S value (1599.5 mg L^{-1}) than the aerobic microbial system did, because the culture in an anaerobic environment has a slower affinity for phenol [40]. The higher K_S value of phenol makes for a lower phenol-affinity with the culture. The K_I value under anaerobic conditions is much higher than that in aerobic conditions, since the culture is less susceptible to phenol inhibition in anaerobic conditions. The K_I value (255.0 mg L^{-1}) obtained from this study also falls in the range of 54.1–799.0 mg L^{-1} for the aerobic environment. The K_I value of our pure culture was close to that of the mixed culture used by Kamali et al. [6].

To determine the yield coefficient (Y) of *P. putida* cells, the experimental results for the initial phenol concentrations (68.3–563.4 mg L^{-1}) in the batch experiments were used. These batch experiments were performed until the initial phenol concentration was fully consumed. The exponential phase was used to calculate the cell concentration produced as a result of consuming phenol. Figure 9 plots the growth yield of *P. putida* cells under various initial phenol and cell concentrations. The growth yield of *P. putida* cells on phenol varied between 0.0585 and 0.600 mg cell/mg phenol. The growth yield of *P. putida* cells

from various batch runs had an average value of 0.592 mg cell/mg phenol, with a standard deviation of 4.995×10^{-3} (Table 3).

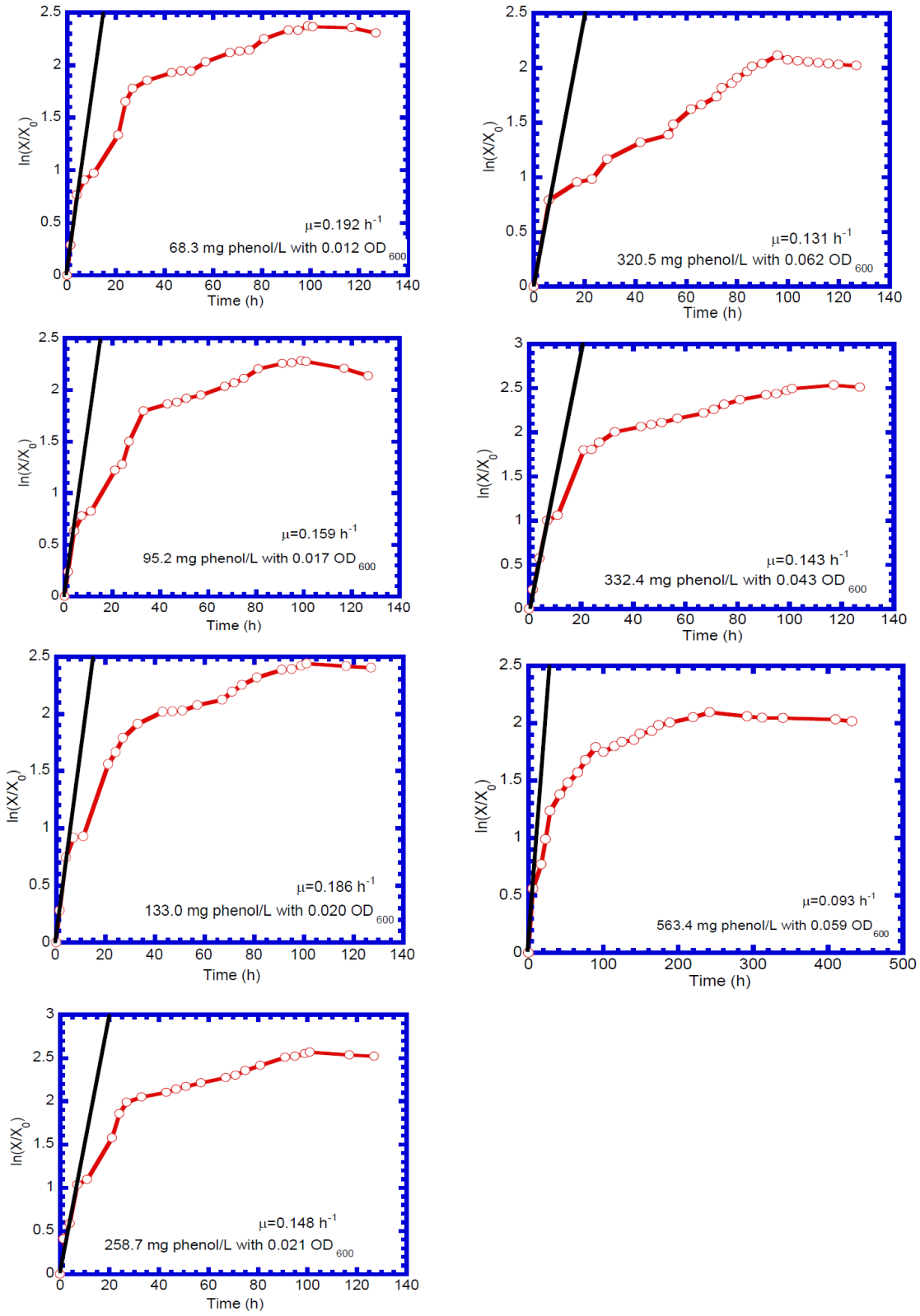

Figure 7. Time profile of growth curves to estimate specific growth rate at logarithmic growth phase, with different initial phenol and cell concentrations.

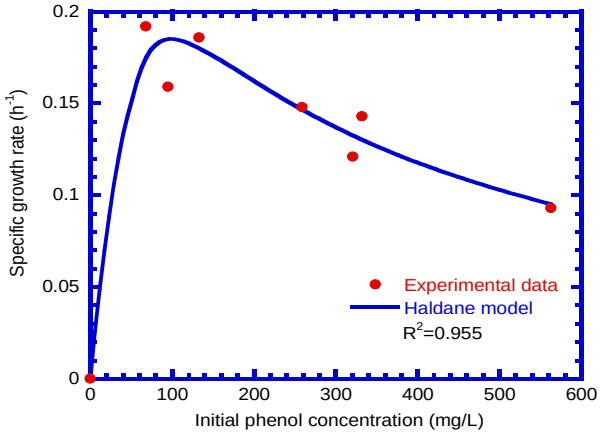

Figure 8. Specific growth rate of cells varied with various initial phenol concentrations. Haldane kinetics was fitted to the experimental data using the least-squares methodology. Maximum specific growth rate (μ_{max}) is 0.31 h^{-1}, phenol half-saturation constant is 26.2 mg/L, and the phenol inhibition constant is 255.0 mg/L.

Table 2. Biokinetic parameters of Haldane kinetics for phenol biodegradation.

Strain	Condition	Initial Phenol Conc. (mg L^{-1})	μ_{max} (h^{-1})	K_S (mg L^{-1})	K_I (mg L^{-1})	References
P. putida (ATCC 49451)	Aerobic	25–800	0.900	6.93	284.3	Wang and Loh [25]
P. putida (DSM 548)	Aerobic	1–100	0.436	6.19	54.1	Monteiro et al. [44]
P. putida F1 (ATCC 700007)	Aerobic	10–200	0.051	18	430	Abuhamed et al. [45]
P. putida (MTCC 1194)	Aerobic	244.4–996.4	0.06	190.8	799.0	Banerjee et al. [46]
P. putida (CCRC 14365)	Aerobic	25–600	0.33	13.9	669	Chung et al. [36]
P. putida (MTCC 1194)	Aerobic	10–1000	0.305	36.33	129.79	Kumar et al. [30]
Mixed culture	Aerobic	23.5–659	0.3095	74.65	648.13	Bajaj et al. [43]
Mixed culture	Aerobic	250–1000	-	692	231	Kamali et al. [6]
Mixed culture	Anaerobic	400–1000	-	1599.5	16,500	Angelucci et al. [40]
P. putida (BCRC 14365)	Aerobic	68.3–563.4	0.31	26.2	255.0	This study

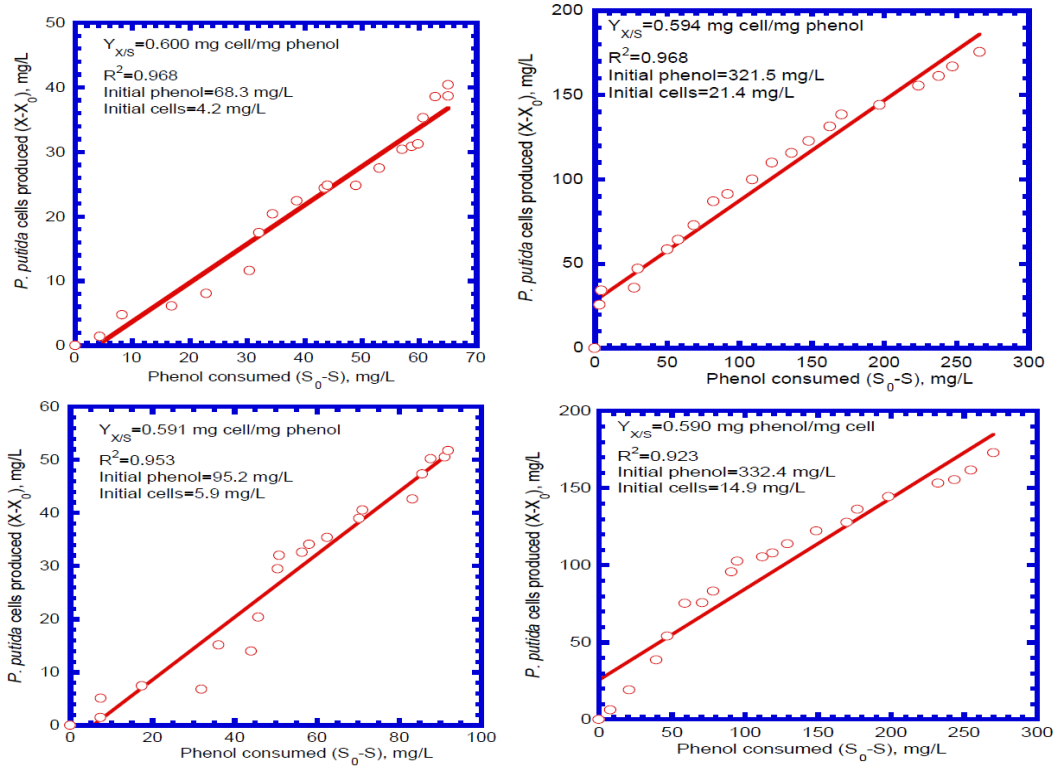

Figure 9. *Cont.*

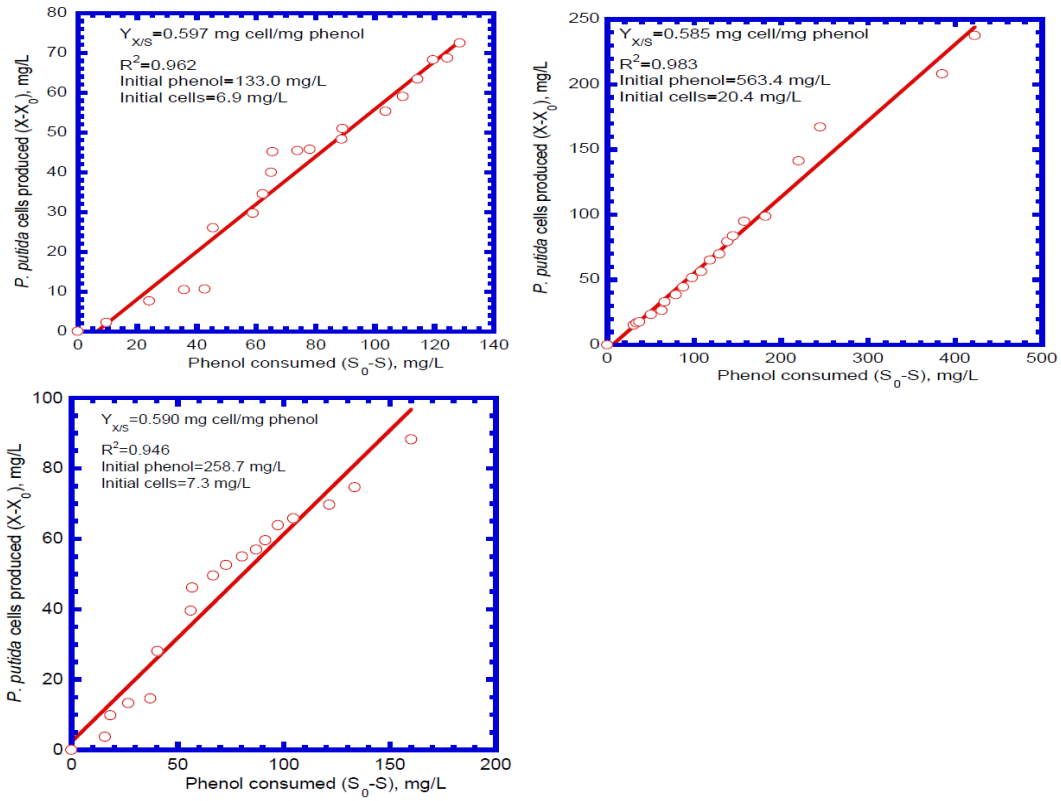

Figure 9. Plot to calculate the yield coefficient (Y) for *P. putida* cells at various initial phenol and cell concentrations.

The experimental data of the endogenous region was plotted as natural logarithm-ln (residual cell concentration) against time to assess the slope that provides the decay coefficient (*b*). Figure 10 shows the seven batch kinetic tests used to evaluate the decay coefficient of *P. putida* cells. The decay coefficient was found to range from 0.0552 to 0.0588 day^{-1}, with an initial phenol concentration of 68.3–563.4 mg/L. The decay coefficients of cells determined from various batch experiments have an average of 5.70×10^{-2}, with a standard deviation of 1.122×10^{-3} (Table 3).

Table 3. Determination of growth yield and decay coefficient of *P. putida* cells.

Run No.	Initial Phenol Concentration (mg L^{-1})	Biokinetic Parameters	
		$Y_{x/s}$, (mg mg^{-1})	*b* (d^{-1})
1	68.3	0.600	5.52×10^{-2}
2	95.2	0.591	5.65×10^{-2}
3	133.0	0.597	5.88×10^{-2}
4	258.7	0.590	5.72×10^{-2}
5	321.5	0.594	5.77×10^{-2}
6	332.4	0.590	5.65×10^{-2}
7	563.4	0.585	5.72×10^{-2}
mean		0.592	5.70×10^{-2}
standard deviation	–	4.995×10^{-3}	1.122×10^{-3}

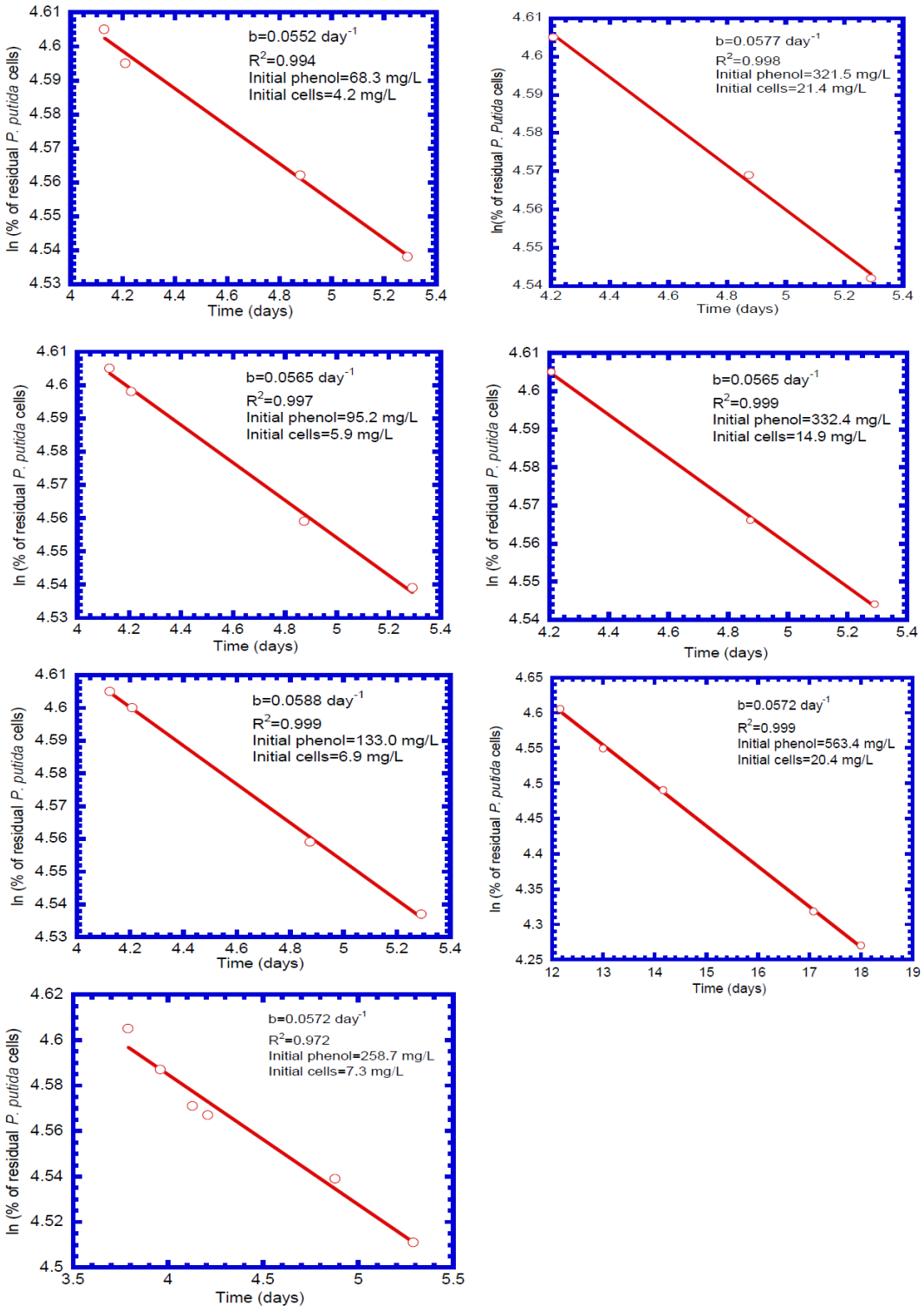

Figure 10. Batch experiments to evaluate the decay coefficient (*b*) for *P. putida* cells.

4.4. Determination of Mass Transfer Coefficients

The value of α was 3.842×10^{-3} L/g for the *P. putida* cells using the technique indicated by Ju and Ho [47]. The diffusivity of glucose as a chemical with low molecular weight is equal to the corresponding value in water for the 2–5% Ca-alginate beads [19]. The diffusivity of phenol (D_s) in 2% Ca-alginate gel beads, applied in a continuous-flow bioreactor, is assumed to be the same value

as that in water. The value of D_s at 30 °C, calculated using the formula of Wilke and Chang [48], is 0.965 $cm^2\ d^{-1}$. The effective diffusivity (D_e) of phenol is 0.236 $cm^2\ d^{-1}$. The values of *Re* and *Sc* are 38.7 and 712.7, respectively. According to calculation by Equation (14), the mass transfer coefficient k_f was equal to 107.1 cm d^{-1}.

4.5. Phenol Biodegradation

In order to verify the kinetic model of the immobilized cells bioreactor described above, the phenol concentrations predicted by the model for bulk liquid were compared with the experimental results under the initial phenol concentration of 25.2 mg/L in the feed. The biokinetic constants used in the kinetic model simulation for the immobilized cells bioreactor were obtained from the batch tests, as reported earlier, for the growth of free cells, while the mass transfer coefficients were estimated using the empirical formula as mentioned above. Table 4 lists all parameters used in the model simulation for the immobilized cells bioreactor.

Table 4. Biokinetic and reactor constants, as well as mass-transfer coefficients used for the model simulation.

Symbol	Parameters Description (Unit)	Value	Remarks
ε	reactor porosity (dimensionless)	0.72	measured
A	surface area of gel beads (cm^2)	3.522×10^4	calculated
b	decay coefficient of cell in gel beads (d^{-1})	5.70×10^{-2}	measured
D_e	effective diffusivity of phenol in the beads ($cm^2\ d^{-1}$)	0.236	calculated
k_f	mass-transfer coefficient of phenol (cm d^{-1})	107.1	calculated
K_I	inhibition constant of phenol (mg L^{-1})	255.0	measured
K_S	half-saturation constant of phenol (mg L^{-1})	26.2	measured
Q	influent flow rate (mL d^{-1})	6.272×10^3	measured
S_{P0}	concentration of phenol in feed (mg L^{-1})	25.2	measured
V	effective working volume (mL)	1.568×10^3	measured
$Y_{x/s}$	growth yield of cell [mg cell (mg phenol)$^{-1}$]	0.592	measured
μ_{max}	maximum specific growth rate of cell (d^{-1})	7.44	measured

Figure 11 illustrates the model-predicted and experimental results of the effluent phenol concentration over time. The effluent curve of the phenol concentration contains three parts. On the first day, the phenol concentration increased abruptly to 86.6 mg/L (0.866 S_{b0}); no significant utilization of phenol occurred. The phenol-concentration curve in the effluent was viewed as a typical dilution curve, which is a property of a completely stirred tank reactor (CSTR), while the bioreactor was filled with only nutrient media at time zero. During a period of 1–5 days, the second part of the phenol concentration curve in the effluent started to deviate from the peak of the dilution curve. The phenol concentration in the effluent leveled off and then rapidly decreased. Apparently, the immobilized cell system notably degraded the phenol over the course of this period, owing to its active growth. The third part of the phenol concentration curve in the effluent ran from day 5 day to day 40. During this time course, the immobilized cells system achieved a steady-state condition, and the phenol concentration in the effluent was approximately 2.3 mg L^{-1} (0.023 S_{b0}). The removal efficiency for phenol was 97.7%. The model prediction was in sufficient agreement with the observed values from experiments, having a correlation coefficient (R^2) of 0.830.

4.6. Flux into Beads

Figure 12a displays the model-predicted flux of phenol diffused from the bulk liquid phase into the gel bead phase. The flux represents the phenol utilization by immobilized cells. At the onset of the experiment, the flux value started at zero, and the immobilized cell growth was negligible. The flux value increased markedly, at a logarithmic rate, after a period of five days, due to the vigorous growth of immobilized cells. During this period, the immobilized cells vigorously degraded the phenol in the beads. Thus, the phenol concentration gradient between the bulk liquid phase and the

beads/liquid interface increased, significantly increasing the flux of phenol into the beads due to the biological activity of cell growth. During days 5–40, the effluent phenol concentration attained a constant steady state value. The flux of phenol attained a maximum constant value of approximately 0.0171 mg cm^{-2} d^{-1}.

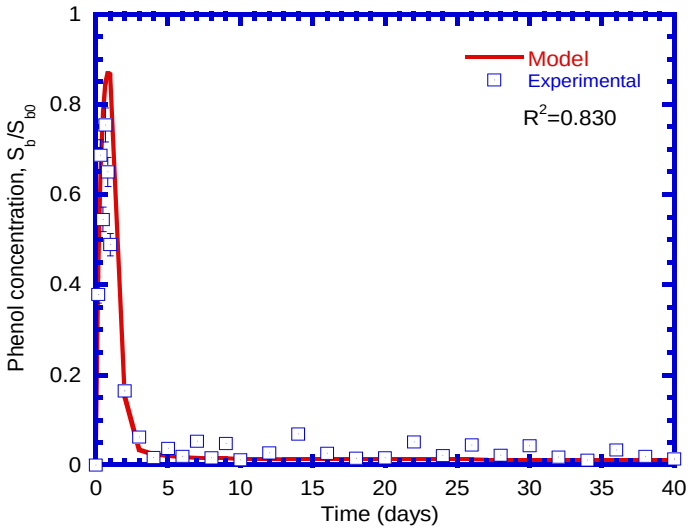

Figure 11. Comparison of experimental data with model simulation for phenol effluent concentration.

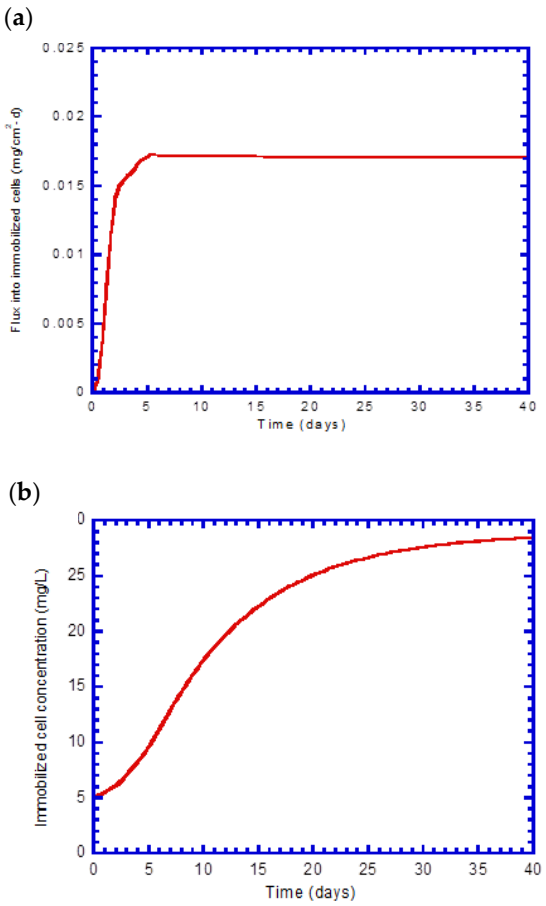

Figure 12. Model prediction versus time of (**a**) phenol flux into beads and (**b**) immobilized cells growth.

4.7. Immobilized Cells Growth

Figure 12b presents the immobilized cells' growth as a function of time via the model's prediction. Apparently, the elapsed time required for immobilized cells to start growing was approximately one day. The model predicted that the immobilized cells actively grew to degrade phenol at a transient-state period of 2–25 days. The maximum value for the growth of immobilized cells was approximately 28 mg L^{-1}.

4.8. Phenol Concentration Profiles

Figure 13a illustrates the time course of phenol at various radial positions within the beads. Initially, there is no phenol when the beads are introduced to the reactor. The diffusion of phenol from the bulk liquid phase to the gel bead phase leads to an abrupt increase in the phenol concentration within the beads. As phenol builds up within the gel beads, the cells start growing and phenol concentration begins to decrease. The cell concentration in the beads increases, until the phenol concentration declines to a lower value in a steady-state condition. No significant difference was found for phenol concentration profiles at different radial positions. The concentration profiles of phenol in the liquid film and bead phase, obtained at 5, 10 and 40 days, are presented in Figure 13b. The phenol diffused through the liquid film into the beads, yielding a concentration profile that was determined by diffusional resistance. Apparently, the radial gradients of phenol concentration increased, as the operating time was increased. On day 5, the system almost reached a steady-state condition. The immobilized cells concentration was approximately 9 mg L^{-1}, and the cells vigorously consumed phenol for growth. On day 10, the phenol concentration decreased rapidly near the center of the beads. On day 40, the phenol concentration profile turned into a curve, indicating a constant phenol flux diffused into the beads at a steady state, and the growth of immobilized cells reached a maximal value.

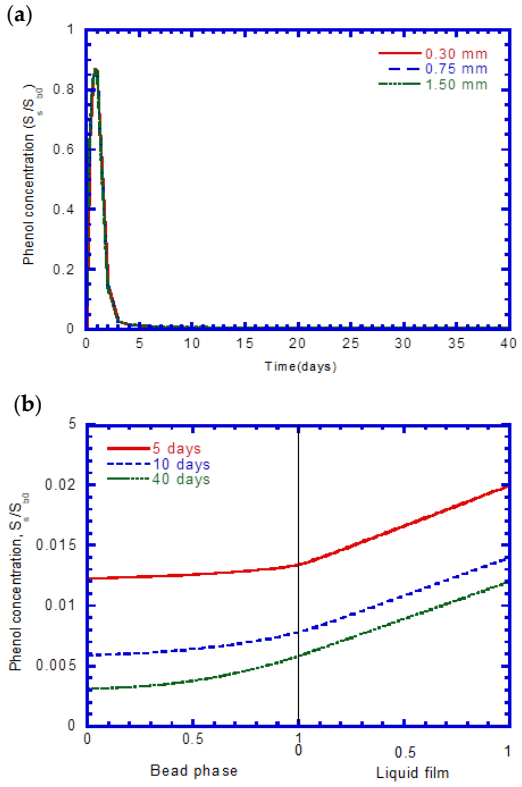

Figure 13. Model predicted phenol concentration profiles (**a**) at different radial positions and (**b**) at different operating times.

4.9. Phenol Removal at Various Loading Rates

The continuous-flow bioreactor with immobilized cells continuously operated at various phenol loading rates of 0.04–0.40 g L^{-1} d^{-1}. Figure 14 illustrates the variation of phenol removal over phenol loading rate. The experimental results revealed that the removal efficiency of phenol was approximately 98% as the phenol loading rate ranged from 0.04 to 0.28 g L^{-1} d^{-1}. However, the phenol removal efficiency abruptly decreased to approximately 10%, while the phenol loading rate increased to 0.32 g L^{-1} d^{-1}. This phenomenon proved that the biodegradation capabilities of *P. putida* immobilized cells were inhibited by phenol at concentrations higher than 800 mg L^{-1}, as the phenol loading rate was 0.28 g L^{-1} d^{-1}. Al-Zuhair and El-NaaS [18] operated a bubble column and spouted bed reactor (SBBR) with immobilized *P. putida* cells in polyvinyl alcohol gel (PVA) particles, to assess the phenol biodegradation efficiency. The experimental results indicated that both bioreactor configurations were effective in the phenol biodegradation, as the inlet initial phenol concentration was 15 g m^{-3}. In their study, the removal efficiency of phenol in SBBR was 100%, however, only approximately 70% phenol removal was attained in the bubble column at a reaction time of 170 h. El-Naas et al. [49] conducted batch experiments to investigate the phenol biodegradation by *P. putida* cells immobilized in polyvinyl alcohol gel pellets, using a bubble column reactor. Their experimental results indicated that a phenol concentration higher than 75 mg L^{-1} inhibited the cell growth, and reduced the biodegradation rate of phenol. A continuous fluidized-bed bioreactor (FBB), with immobilized cells of *P. putida* ATCC 17484 in calcium-alginate gel beads, was conducted to estimate phenol biodegradation at pH 6.6, a temperature of 30 °C, and airflow 43 L air L volume^{-1} min^{-1} [50]. The effective working volume was 3 L. The immobilized cells of *P. putida* in a fluidized-bed continuous mode exhibited a phenol removal efficiency higher than 90%, with a high loading rate of 0.5 g phenol L^{-1} d^{-1} [50]. Their experimental results indicated that FBB had a higher resistance to phenol organic loading rate in influent than the continuous-flow moving-bed bioreactor. However, the removal efficiency of phenol greater than 98% shown in this study is comparable to that attained in the study of González et al. [50].

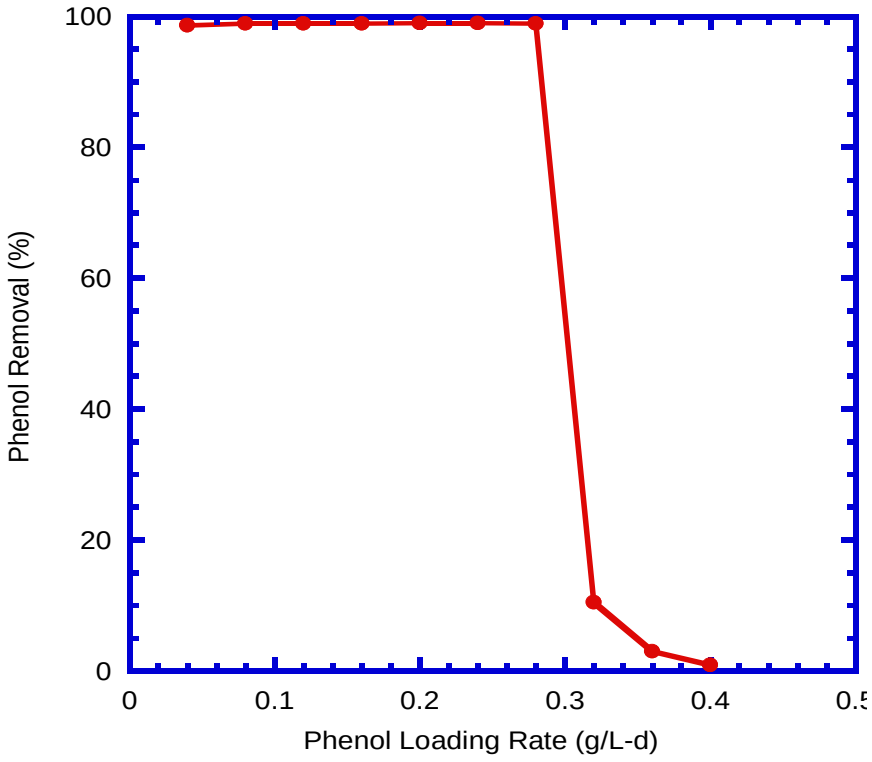

Figure 14. Effect of phenol loading rate on phenol removal in the continuous-flow bioreactor.

5. Conclusions

Phenol degradation by *Pseudomonas putida* BCRC 14365 was investigated at 30 °C and with a pH range of 5.0–9.0 in the batch tests. Experimental results demonstrated that the maximum phenol degradation rate occurred at an initial pH of 7 with suspended and immobilized cells. The peak values of phenol degradation by the free and immobilized cells were 2.84 and 2.64 mg/L-h, respectively, at the optimal pH of 7. At the temperature range of 25–40 °C, and pH 7, the removal efficiencies of phenol degradation at the final stage were 59.3–92% and 87.5–92%, for free and immobilized cells, respectively. The optimal temperature was 30 °C for free and immobilized cells, with the highest phenol removal efficiency of 92%. Seven batch experiments were carried out to determine the biokinetic constants (K_S, K_I, $Y_{X/S}$, and b) by fitting the experimental data into a Haldane equation. The biokinetic constants obtained from the batch experiments were used as input values for model simulation. A kinetic model for describing the phenol degradation by immobilized cells in a continuous-flow moving-bed bioreactor was derived. A continuous-flow moving-bed bioreactor with immobilized cells in calcium alginate beads was constructed to validate the kinetic model. The experimental results demonstrated that the immobilized cell process yields a high removal efficiency for phenol degradation, which was approximately 97.7% at a steady-state condition. The model-predicted results agreed with the experimental results for the effluent concentration of phenol. The flux that diffused from the bulk liquid phase into the liquid film/bead interfaceincreased rapidly as the immobilized cells grew vigorously during the transient-state period. The experimental approach and kinetic model developed in this study can be employed in the design of a pilot-scale or full-scale immobilized cell process for the biodegradation of phenolic wastewater in various industries.

Author Contributions: Y.-H.L. conceived and designed the experiments, developed and solved the kinetic model and analyzed the experimental data; Y.-S.C. conducted the experiments and collected the experimental data. All authors have read and agreed to the published version of the manuscript.

Funding: This research was funded by Ministry of Science and Technology of Taiwan under Contract No. MOST 106-2221-E-166-001-MY2.

Conflicts of Interest: The authors declare no conflict of interest.

References

1. Dionisi, D.; Etteh, C.C. Effect of process conditions on the aerobic biodegradation of phenol and paracetamol by open mixed microbial cultures. *J. Environ. Chem. Eng.* **2019**, *7*, 1–8. [CrossRef]
2. Papazi, A.; Pappas, I.; Kotzabasis, K. Combinational system for biodegradation of olive oil mill wastewater phenolics and high yield of bio-hydrogen production. *J. Biotechnol.* **2019**, *306*, 47–53. [CrossRef] [PubMed]
3. Zhang, C.; Bennett, G.N. Biodegradation of xenobiotic by anaerobic bacteria. *Appl. Microbiol. Biotechnol.* **2005**, *67*, 600–618. [CrossRef]
4. Geng, A.; En-WeiSoh, A.; Lim, C.J.; Loke, C.T.L. Isolation and characterization of a phenol-degrading bacterium from an industrial activated sludge. *Appl. Microbiol. Biotechnol.* **2006**, *71*, 728–735. [CrossRef] [PubMed]
5. Jiang, Y.; Deng, T.; Shang, Y.; Yang, K.; Wang, H. Biodegradation of phenol by entrapped cell of *Debaryomyces* sp. with nano-Fe_3O_4 under hypersaline conditions. *Int. Biodeterior. Biodegrad.* **2017**, *123*, 37–45. [CrossRef]
6. Kamali, M.; Gameiro, T.; Costa, M.E.; Capela, I.; Aminabhavi, T.M. Enhanced biodegradation of phenolic wastewaters with acclimated activated sludge—A kinetic study. *Chem. Eng. J.* **2019**, *378*, 1–7. [CrossRef]
7. Dong, R.; Chen, D.; Li, N.; Xu, Q.; Li, H.; He, J.; Lu, J. Removal of phenol from aqueous solution using acid-modified *Pseudomonas putida*-sepiolite/ZIF-8 bio-nanocomposites. *Chemosphere* **2020**, *239*, 1–11. [CrossRef]
8. Li, H.; Meng, F.; Duan, W.; Lin, Y.; Zhang, Y. Biodegradation of phenol in saline or hypersaline environments by bacteria: A review. *Ecotoxicol. Environ. Saf.* **2019**, *184*, 1–9. [CrossRef]
9. Chae, Y.; Kim, D.; Cui, R.; Lee, J.; An, Y.J. Deriving hazardous concentrations of phenol in soil ecosystems using a species sensitivity distribution approach. *J. Hazard. Mater.* **2020**. [CrossRef]

10. Afsharnia, M.; Saeidi, M.; Zarei, A.; Narooie, M.R.; Biglari, H. Phenol removal from aqueous environment by adsorption onto pomegranate peel carbon. *Electron. Phys.* **2016**, *8*, 3248–3256. [CrossRef]
11. Quan, X.; Shi, H.; Liu, H.; Wang, J.; Qian, Y. Removal of 2,4-dichlorophenol in a conventional activated sludge system through bioaugmentation. *Process Biochem.* **2004**, *39*, 1701–1707. [CrossRef]
12. Atlow, S.C.; Bonadonna-Aparo, L.; Klibanov, A.M. Dephenolization of industrial wastewaters catalyzed by polyphenol oxidase. *Biotechnol. Bioeng.* **1984**, *6*, 599–603. [CrossRef] [PubMed]
13. Verma, S.R.; Tonk, I.P.; Gupta, A.K.; Saxena, M. Evaluation of an application factor for determining the safe concentration of agricultural and industrial chemicals. *Water Res.* **1984**, *18*, 111–115. [CrossRef]
14. Kim, J.S.; Chin, P. Acute and chronic toxicity of phenol to mysid, *Archaeomysis kokuboi*. *Korean J. Fish. Aquat. Sci.* **1995**, *28*, 87–97.
15. Banerjee, A.; Ghoshal, A.K. Phenol degradation performance by isolated *Bacillus cereus* immobilized in alginate. *Int. Biodeterior. Biodegrad.* **2011**, *65*, 1052–1060. [CrossRef]
16. Parvanova-Mancheva, T.; Vasileva, E.; Beschkov, V.; Gerginova, M.; Stoilova-Disheva, M.; Alexieva, Z. Biodegradation potential of *Pseudomonas putida* to phenol compared to xanthobacter autotrophicus GJ10 and *Pseudomonas denitrificans* strains. *J. Chem. Technol. Metall.* **2020**, *55*, 23–27.
17. Kurzbaum, E.; Raizner, Y.; Cohen, O.; Suckeveriene, R.Y.; Kulikov, A.; Hakimi, B.; Kruh, L.I.; Armon, R.; Farber, Y.; Menashe, O. Encapsulated *Pseudomonas putida* for phenol biodegradation: Use of a structural membrane for construction of a well-organized confined particle. *Water Res.* **2017**, *121*, 37–45. [CrossRef]
18. Al-Zuhair, S.; El-Naas, M. Immobilization of *Pseudomonas putida* in PVA gel particles for biodegradation of phenol at high concentrations. *Biochem. Eng. J.* **2011**, *56*, 46–50. [CrossRef]
19. Tanake, H.; Matsumura, M.; Veliky, I.A. Diffusion characteristics of substrates in Ca-alginate gel beads. *Biotechnol. Bioeng.* **1984**, *26*, 53–58. [CrossRef]
20. Aksu, Z.; Bülbül, G. Determination of the effective diffusion coefficient of phenol in Ca-alginate-immobilized *P. putida* beads. *Enzyme Microb. Technol.* **1999**, *25*, 344–348. [CrossRef]
21. Zulfadhly, Z.; Mashitah, M.; Bhatia, S. Heavy metals removal in fixed-bed column by the macro fungus *Pycnoporus sanguineus*. *Environ. Pollut.* **2001**, *112*, 463–470. [CrossRef]
22. Wu, J.; Yu, H. Biosorption of 2,4-dichlorophenol from aqueous solutions by immobilized Phanerochaete chrysosporium biomass in a fixed-bed column. *Chem. Eng. J.* **2008**, *138*, 128–135. [CrossRef]
23. Febrianto, J.; Kosasih, J.; Sunarso, Y.; Ju, N. Equilibrium and kinetic studies in adsorption of heavy metals using biosorbent: A summary of recent studies. *J. Hazard. Mater.* **2009**, *162*, 616–645. [CrossRef] [PubMed]
24. Xiao, M.T.; Huang, Y.Y.; Ye, J.; Guo, Y.H. Study on the kinetic characteristics of the asymmetric production of R-(−)-mandelic acid with immobilized *Saccharomyces cerevisiae* FD11b. *Biochem. Eng. J.* **2008**, *39*, 311–318. [CrossRef]
25. Wang, S.J.; Loh, K.C. Modeling the role of metabolic intermediates in kinetics of phenol biodegradation. *Enzyme Microb. Technol.* **1999**, *25*, 177–184. [CrossRef]
26. Onysko, K.A.; Budman, H.M.; Robinson, C.W. Effect of temperature on the inhibition kinetics of phenol biodegradation by *Pseudomonas putida* Q5. *Biotechnol. Bioeng.* **2000**, *70*, 291–299. [CrossRef]
27. Vinod, A.V.; Reddy, G.V. Simulation of biodegradation process of phenolic wastewater at higher concentrations in the fluidized-bed bioreactor. *Biochem. Eng. J.* **2005**, *24*, 1–10. [CrossRef]
28. Reardon, K.F.; Mosteller, D.C.; Rogers, J.D.B. Biodegradation kinetics of benzene, toluene, and phenol as single and mixed substrates for *Pseudomonas putida* F1. *Biotechnol. Bioeng.* **2000**, *69*, 386–400. [CrossRef]
29. Chung, T.P.; Wu, C.Y.; Juang, R.S. Improved dynamic analysis on cell growth with substrate inhibition using two-phase models. *Biochem. Eng. J.* **2005**, *25*, 209–217. [CrossRef]
30. Kumar, A.; Kumar, S.; Kumar, S. Biodegradation kinetics of phenol and catechol using *Pseudomonas putida* MTCC 1194. *Biochem. Eng. J.* **2005**, *22*, 151–159. [CrossRef]
31. Wakao, N.; Smith, J.M. Diffusion and reaction in porous catalysts. *Ind. Eng. Chem. Fund.* **1964**, *2*, 123–127. [CrossRef]
32. Korgel, B.A.; Rotem, A.; Monbonquett, H.G. Effective diffusivity of galactose in calcium alginate gels containing immobilized *Zymonmonas mobilis*. *Biotechnol. Prog.* **1992**, *8*, 111–117. [CrossRef] [PubMed]
33. Brian, P.L.T.; Hales, H.B. Effect of transpiration and changing diameter on heat and mass transfer to sphere. *AIChE J.* **1969**, *15*, 419–425. [CrossRef]
34. Juang, R.S.; Tsai, S.Y. Growth kinetics of *Pseudomonas putida* in the biodegradation of single and mixed phenol and sodium salicylate. *Biochem. Eng. J.* **2006**, *31*, 133–140. [CrossRef]

35. Tsai, S.Y.; Juang, R.S. Biodegradation of phenol and sodium salicylate mixtures by suspended *Pseudomonas putida* CCRC 14365. *J. Hazard. Mater.* **2006**, *138*, 125–132. [CrossRef]
36. Chung, T.P.; Tseng, H.Y.; Juang, R.S. Mass transfer effect and intermediate detection for phenol degradation in immobilized *Pseudomonas putida* systems. *Process Biochem.* **2003**, *38*, 1497–1507. [CrossRef]
37. Faridnasr, M.; Ghanbari, B.; Sassani, A. Optimization of the moving-bed biofilm sequencing batch reactor (MBSBR) to control aeration time by kinetic computational modeling: Simulated sugar-industry wastewater treatment. *Bioresour. Technol.* **2016**, *208*, 149–160. [CrossRef]
38. Rosenkranz, F.; Cabrol, L.; Carballa, M.; Donoso-Bravo, A.; Cruz, L.; Ruiz-Filippi, G.; Chamy, R.; Lema, J.M. Relationship between phenol degradation efficiency and microbial community structure in an anaerobic SBR. *Water Res.* **2013**, *47*, 6739–6749. [CrossRef]
39. Vital-Jacome, M.; Buitrón, G.; Moreno-Andrade, I.; Garcia-Rea, V.; Thalasso, F. Microrespirometric determination of the effectiveness factor and biodegradation kinetics of aerobic granules degrading 4-chlorophenol as the sole carbon source. *J. Hazard. Mater.* **2016**, *313*, 112–121. [CrossRef]
40. Angelucci, D.M.; Clagnan, E.; Brusetti, L.; Tomei, M.C. Anaerobic phenol biodegradation: Kinetic study and microbial community shifts under high-concentration dynamic loading. *Appl. Microbiol. Biotechnol.* **2020**. [CrossRef]
41. Sahinkaya, E.; Dilek, F.B. Effects of 2,4-dichlorophenol on activated sludge. *Appl. Microbiol. Biotechnol.* **2002**, *59*, 361–367. [PubMed]
42. Pirbazari, M.; Ravindran, V.; Badriyha, B.N.; Kim, S.H. Hybrid membrane filtration process for leachate treatment. *Water Res.* **1996**, *30*, 2691–2706. [CrossRef]
43. Bajaj, M.; Gallert, C.; Winter, J. Phenol degradation kinetics of an aerobic mixed culture. *Biochem. Eng. J.* **2009**, *46*, 205–209. [CrossRef]
44. Monteiro, Á.A.; Boaventura, R.A.; Rodrigues, A.E. Phenol biodegradation by *Pseudomonas putida* DSM 548 in a batch reactor. *Biochem. Eng. J.* **2000**, *6*, 45–49. [CrossRef]
45. Abuhamed, T.; Bayraktar, E.; Mehmetoğlu, T.; Mehmetoğlu, Ü. Kinetics model for growth of *Pseudomonas putida* F1 during benzene, toluene and phenol biodegradation. *Process Biochem.* **2004**, *39*, 983–988. [CrossRef]
46. Banerjee, I.; Modak, J.M.; Bandopadhyay, K.; Das, D.; Maiti, B.R. Mathematical model for evaluation of mass transfer limitations in phenol biodegradation by immobilized *Pseudomonas putida*. *J. Biotechnol.* **2001**, *87*, 211–223. [CrossRef]
47. Ju, L.K.; Ho, C.S. Correlation of cell volume fractions with cell concentrations in fermentation media. *Biotechnol. Bioeng.* **1988**, *32*, 95–99. [CrossRef]
48. Wilke, C.E.; Chang, P. Correlation of diffusion coefficients in dilute solutions. *AIChE J.* **1955**, *1*, 264–270. [CrossRef]
49. El-Naas, M.H.; Al-Muhtaseb, S.A.; Makhlouf, S. Biodegradation of phenol by *Pseudomonas putida* immobilized in polyvinyl alcohol (PVA) gel. *J. Hazard. Mater.* **2009**, *164*, 720–725. [CrossRef]
50. González, G.; Herrera, G.; García, M.T.; Peña, M. Biodegradation of phenolic industrial wastewater in a fluidized bed bioreactor with immobilized cells of *Pseudomonas putida*. *Bioresour. Technol.* **2001**, *80*, 137–142. [CrossRef]